PAPER

Information Gathering for Wireless Sensor Networks with Information Converting to Wireless Physical Parameters

Tomomi ENDOU[†a)], Shunta SAKAI[†b)], *Student Members*, *and* Takeo FUJII[†c)], *Member*

SUMMARY Recently, the growing concepts that information communication technologies apply to social infrastructures have caused deep interests with *wireless sensor networks* (WSNs). WSNs can be used for various application areas such as home, health, factory and so on. For the different application areas, there are different technical issues (e.g., security, reliability, real time gathering, long life time, scalability). Efficient information gathering can be potentially obtained if we take a suitable information gathering method with considering the requirements of each WSN application. Thus, we have not persisted all information gathering perfectly and have proposed one of simple information gathering methods in response to the requirements of WSN applications in this paper. In the proposed method, the information is converted to physical-layer parameters of wireless communications, such as frequency and time. Also, simulations are performed to validate the effectiveness of the proposed method in real time gathering and estimating with high precision.
key words: *wireless sensor networks, information gathering, real time communication, OFDM signal*

1. Introduction

Recently, the growing concepts that information communication technologies apply to social infrastructures, such as smart grid and smart city, have caused deep interests with *wireless sensor networks* (WSNs) [1], [2]. WSNs are a class of ad-hoc networks established by *a fusion center* (FC) and multiple autonomous devices like nodes, routers, gateway where each node is connected to sensors. In WSNs, the fusion center is reliably powered and monitors environmental conditions by gathering information from autonomous sensor nodes. Each sensor node is a low-cost device powered by a battery and has a function of sensing surrounding environment, performing simple processing tasks and sending information over wireless communications. This makes it easy to be attached at any location and to construct any networks. Such flexibility greatly eases costs and efforts for deployment and maintenance. Therefore WSNs have been applied to a wide range of applications in the recent few years. For example, smart city [3], smart home [4], wildlife habitat monitoring [5], and environmental research [6], to mention only a few, have been developed.

At the present time, the standardized protocols for information gathering, such as IEEE802.15.4/ZigBee and

specified low power radio (SLPR), have been used mainly as a wireless communication system in WSNs. The standards are based on generic packet communications that sensor nodes send the information by packets storing data in turn using *carrier sense multiple access with collision avoidance* (CSMA/CA). Since the larger number of sensor nodes is arranged, the more overhead of protocols for avoiding interferences is necessary, and the longer the period required for gathering information from all sensor nodes becomes, these standards are not suitable for gathering information from a large number of sensor nodes in real time. Moreover, the signal processing of packet communications causes the problems of electric power consumption of sensor nodes. In conventional WSNs, there are many studies using the standards based on generic packet communications with the aim of reliable communication under the restriction of the power and cost of sensor nodes. However, the requirements of each WSN application are various such as security, reliability, real time gathering, long life time, scalability and so on. For example, to monitor a spatial distribution of temperature, the fusion center only comprehends the statistical property of the temperature distribution. In this case, it is not required to gather the information from all sensor nodes with high precision.

We consider that the various characteristics of WSN applications may improve the efficiency of information gathering by changing wireless transmission method. From these points of view, we do not care all information gathering perfectly and have proposed the simple information gathering methods in response to the requirements of each WSN application [7]–[10]. In these methods, the fusion center gathers the information from sensor nodes by converting the information to physical-layer parameters of wireless communication. The wireless transmission method using *orthogonal frequency division multiple* (OFDM) subcarrier mapping in [7] is for the information gathering in cooperative sensing of cognitive radio. The cooperative nodes around the master node convert the test statistic of energy detection to a subcarrier frequency of OFDM signals and transmit the tone signals with the converted subcarrier frequency at the same time. The master node effectively gathers the different information from the multiple cooperative nodes at once. In this paper, we propose the method for gathering the positional data of sensor nodes in addition to the sensed data based on OFDM subcarrier mapping [10]. In the proposed method, the two-dimensional distribution of an observation object, the sensed data and the positional data,
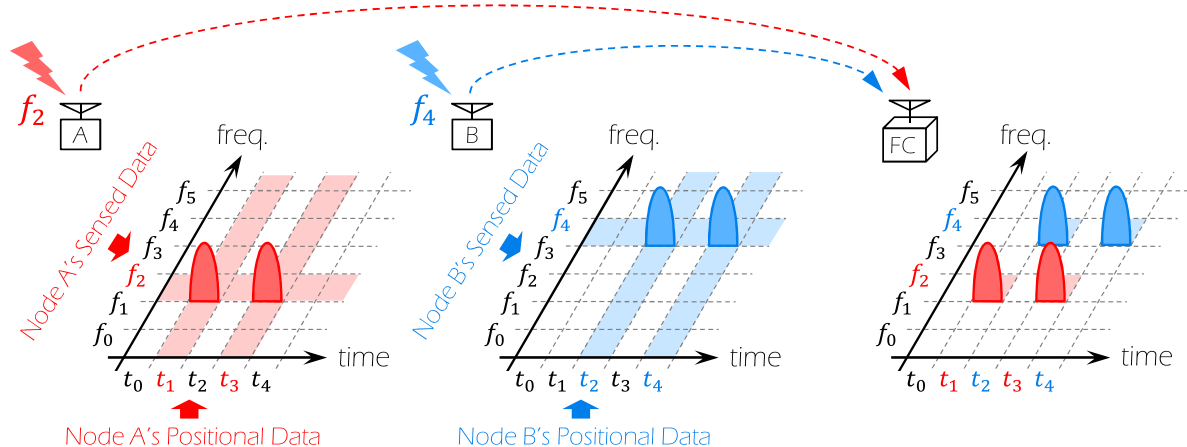
Fig. 1 Process of proposed information gathering method.

is gathered from multiple sensor nodes by converting the sensed data and the positional data to frequency-axis (subcarrier frequency) and time-axis (time slots), respectively. Each sensor node sends the information by transmitting the tone signals with the subcarrier frequency mapped to own sensed data at the time slots mapped to own positional data. Although the proposed method only requires simpler communications than the standards based on generic packets communications, the received signals may include the false data in addition to the correct data sent by sensor nodes. That is because that the relation between the positional data and time slots is not unique for mitigating the period required for information gathering. Thus, we propose the five methods for estimating the distribution information sent by sensor nodes.

The rest of the paper is organized as follows: we present the proposed method for information gathering and explain how to convert the information to physical-layer parameters and how to estimate the distribution information sent by sensor nodes in Sect. 2. In Sect. 3, we discuss the relation between the estimation accuracy and the spatial correlation of an observation object and theoretically analyze the proposed methods. In Sect. 4, we evaluate the performance of the proposed method. Finally, a conclusion is given in Sect. 5.

2. Proposed Method

In this section, we explain how to gather the two-dimensional distribution of an observation object by using the proposed method. At the beginning, the outline and process of the proposed method is described. Next, we describe how to convert the information to the physical-layer parameters. Then, the method of information recovery from the received signals at the fusion center is shown, and we indicate the necessity of the information estimation. Finally, we explain the five methods for estimating the distribution information sent by sensor nodes.

2.1 Outline of Proposed Method

The following items are the process of the proposed method and the system image is shown in Fig. 1.

  i. The fusion center sends the request packets to all sensor nodes for setting up the information gathering. The parameters of the information converting, the frequency mapping and the timing mapping, are notified to sensor nodes by the request packets.
 ii. Each sensor node receives the request packets and synchronizes frequency and time clocks by utilizing the received packets.
iii. In each sensor node, own sensed data is converted to a subcarrier frequency, and own positional data is also converted to two time slots. (Sect. 2.2)
 iv. Each sensor node transmits the tone signal, continuous waves, using the mapped subcarrier frequency at the mapped two time slots.
  v. The tone signals aggregating in the wireless channel, the fusion center receives a part of OFDM signals.
 vi. At the fusion center, the subcarriers of the received signals are detected by an energy detector at each time slot.
vii. The fusion center estimates the information by using the combination between the detected subcarriers and time slots. (Sect. 2.3)

In the proposed method, the sensed data is mapped to a subcarrier frequency of OFDM signals. Therefore, various sensed data can be gathered from multiple sensor nodes at the same time due to the orthogonality of OFDM subcarrier frequency. Moreover, the proposed method is simpler wireless communications system than generic packet communications with modulation and demodulation. As a result, the proposed method is expected to shorten the period required for information gathering and to reduce the processing task and the battery power consumption of each sensor node.

The proposed method requires accurate synchronization on frequency and time in the WSN, since the frequencies and time of wireless signals are information itself. In

the past decade, there have been rich research results on distributed synchronization for WSN [11]. Among them, *the reference broadcasting synchronization protocol* (RBS) has been first proposed as time synchronization protocol in [12]. To improve the accuracy of synchronization and to reduce the numbers of message exchanges in RBS, *the timing-sync protocol for sensor networks* (TPSN) has been proposed in [13] which requires only two message exchanges for each sensor node in the WSN. By utilizing pilot symbols or training sequences (e.g., [14], [15]), time-frequency synchronization among a set of receivers is ensured without requiring complicated computations. We consider that the proposed method can ensure the synchronization by using the existing protocol and assume that time-frequency synchronization in the WSN is perfect in this paper.

2.2 Information Conversion to Wireless Parameters

2.2.1 Frequency Mapping of Sensed Data

In the proposed method, the sensed data of each sensor node is sent to the fusion center by converting to OFDM subcarrier frequency. The frequency mapping image is shown in Fig. 2 and the frequency mapping functions are given by:

$$n_{\text{freq}} = \begin{cases} N_{\min} & (k_i \le K_{\min}) \\ \left\lfloor \frac{W + k_i - K_{\text{mid}}}{A} \right\rfloor & (K_{\min} < k_i < K_{\max}) \,, \\ N_{\max} & (K_{\max} \le k_i) \end{cases} \quad (1)$$

where n_{freq} denotes subcarrier number of OFDM signals, k_i means sensed data value of ith sensor node. $N_{\min}$ and $N_{\max}$ are the minimum and maximum number of OFDM subcarriers used for the frequency mapping, respectively. A indicates the quantization level of the sensed data. $[K_{\min}, K_{\max}]$ and $2W$ are the range and width of gathered value with A

precision. K_{mid} means the middle value of $[K_{\min}, K_{\max}]$. Each sensor node chooses one of above mapping functions (1) according to their sensed data value and converts sensed data value to a subcarrier number. If $k_i \le K_{\min}$, the ith sensor node selects the $N_{\min}$th subcarrier. If $k_i \ge K_{\max}$, the ith sensor node selects the $N_{\max}$th subcarrier. If $K_{\min} < k_i < K_{\max}$, the ith sensor node converts k_i to subcarrier number with A precision. The sensed data in the range of $[K_{\min}, K_{\max}]$ with A precision is gathered by above mapping. Figure 2 shows that the sensed data in the range of $[20.0, 30.0]°$C is converted to a subcarrier number in the range of $[0, 100]$ with $0.1°$C precision. Due to $k_A \le 20.0°$C, Node A chooses 0th subcarrier frequency f_0. Similarly, due to $k_E \ge 30.0°$C, Node E chooses 100th subcarrier frequency f_{100}. Owing to $20.0°$C $< k_B, k_C, k_D < 30.0°$C, Node B,C,D convert each sensed data to f_1, f_{50}, f_{98}.

2.2.2 Timing Mapping of Positional Data

The quantized positional data (x, y) is sent by converting to two time slots of the signal transmission in the proposed method. The timing mapping image is shown in Fig. 3. The sensing field is partitioned into $X \times Y$ cells, and the $X \times Y$ cells are grouped by $\alpha \times \alpha$ cells. α decides the group size in the timing mapping. The x-axis and y-axis of each group are mapped α time slots respectively, that is, each cell is mapped to two time slots. The timing mapping functions are given by:

$$n_{\text{time},x} = 2Y g_x + 2\alpha g_y + c_x \quad (2)$$

$$n_{\text{time},y} = 2Y g_x + 2\alpha g_y + c_y + \alpha \quad (3)$$

$$g_x = \lfloor x/\alpha \rfloor \qquad\qquad g_y = \lfloor y/\alpha \rfloor$$

$$c_x = x \bmod \alpha \qquad\qquad c_y = y \bmod \alpha,$$

where $n_{\text{time},x}, n_{\text{time},y}$ denote time slot number mapped to
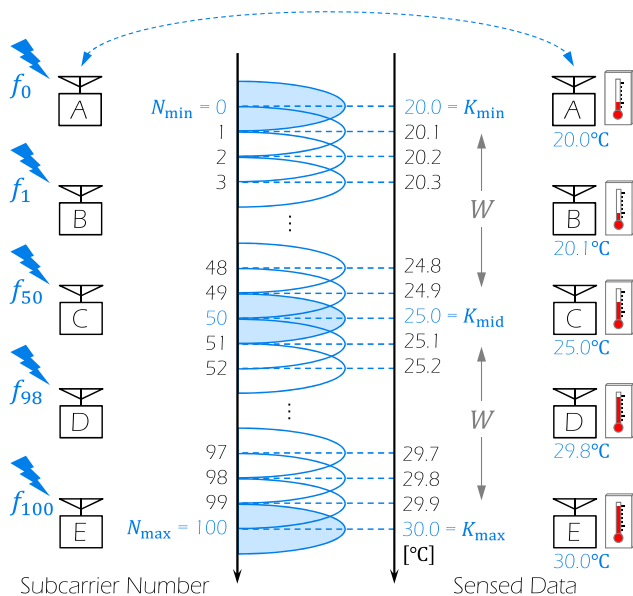
Fig. 2 Frequency mapping of sensed data.
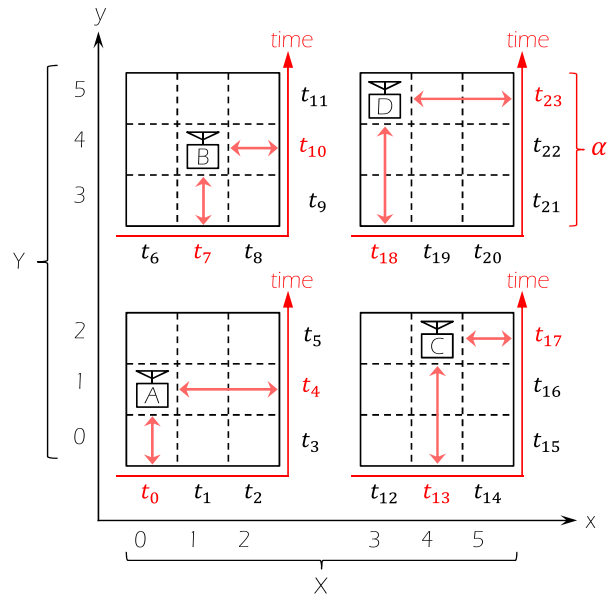
Fig. 3 Timing mapping of positional data.

(x, y). g_x, g_y mean the group position and c_x, c_y mean the coordinates on the group, that is, the positional data (x, y) is represented as the coordinates (c_x, c_y) on the group (g_x, g_y). According to the above mapping functions, each sensor node transforms own position (x, y) to the group position (g_x, g_y) and the coordinates (c_x, c_y) on the group. Then, each sensor node converts the positional data to the time slots of the signal transmission using the mapping function (2),(3) and the parameters X, Y, α noticed by the fusion center at the start of the information gathering. At the $n_{\text{time},x}, n_{\text{time},y}$th time slots mapped to respective own positional data, sensor nodes transmit the tone signals. For example, Node A at $(0,1)$ transmits the tone signals at the 0,4th time slots t_0, t_4 in Fig. 3. Node B at $(1,4)$ transmits at the 7,10th time slots t_7, t_{10}. In the above mapping, 2α slots are required for the assignment of one group composed of $\alpha \times \alpha$ cells. While each cell is simply mapped to a different time slot each, α^2 slots are needed. The number of time slots for the proposed mapping is $\frac{2}{\alpha}$ times fewer than that for the later simple mapping. Further, the larger the group size α is, the shorter it can take time to gather the information in the proposed mapping as shown in the example in Fig. 4. However, it is necessary that the fusion center estimates the information sent by sensor nodes since a relation between the positional data and time slots is not unique unlike the frequency mapping.
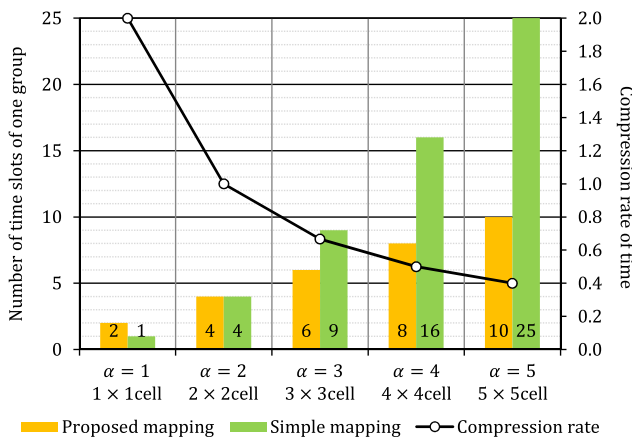
Fig. 4 Compression of time slots requiered for timing mapping.

2.3 Information Estimation

In this subsection, we explain how to estimate the distribution information at the fusion center. At the beginning, how to extract the information from the received tone signals and the necessity for the information estimation are described. Next, we propose the five methods to estimate the distribution information. These methods are listed in Table 1 and can be roughly divided into two types. One type, *the averaging estimation method* (AE method), utilizes a spatial correlation of an observation object. The other type, *the likelihood estimation method* (LE method), utilizes the node location and estimates preferentially the information likely to be sent by sensor nodes.

2.3.1 Information Extraction from Received Signals

The process of the information extracting from the received tone signals is as follows. First, the subcarriers of the received signals are detected by using an energy detector at each time slot. If an average received power of a subcarrier is higher than a threshold, the detected subcarrier frequency component is regarded as that sent by sensor nodes. Next, the fusion center judges the common subcarriers of each cell according to the combination between the detected subcarriers and time slots. Out of the subcarrier frequency components detected at the $n_{\text{time},x}, n_{\text{time},y}$th time slots mapped to (x, y), the same subcarrier frequency components are defined as the common subcarriers. If the energy detection is perfect, the common subcarriers certainly contain the frequency components sent by sensor nodes. Then the common subcarrier number $n_{\text{com}}(x, y)$ is converted to sensed data value $k_{\text{est}}(x, y)$ by the inverse frequency mapping. The inverse mapping function is given by:

$$k_{\text{est}}(x, y) = An_{\text{com}}(x, y) - W + K_{\text{mid}}. \tag{4}$$

Figure 5 shows the example of the information extraction when Nodes A~E are attached and send the information as shown in Fig. 5(a). Here, we suppose that the energy detection at the fusion center is perfect. When Node A~E send the information using the proposed method, the received signals at the fusion center is shown in Fig. 5(b). Figure 5(c)

<p align="center">Table 1 Characteristic of each estimation method.</p>

Characteristic	AE (1)	AE (2)	LE (1)	LE (2)	LE (3)
Averaging estimation: the information is estimated by only averaging. This method is very simple and required for a low processing task.	√	√	(√)	(√)	(√)
Likelihood estimation: the information likely to be sent by sensor nodes is preferentially estimated.	-	-	√	√	√
Prior information: the node location is utilized for the estimation, that is, the fusion center should gather the location information of sensor nodes in advance.	-	√	-	-	√
Limited node location: the effective situation is only when one cell has one or few sensor nodes.	-	-	√	√	-
Utilizing spatial correlation: the higher the spatial correlation of the observation object becomes, the more effective this method is.	√	√	-	-	-

Fig. 5 Information extraction from received signals.

Fig. 6 Priority cells of each LE method.
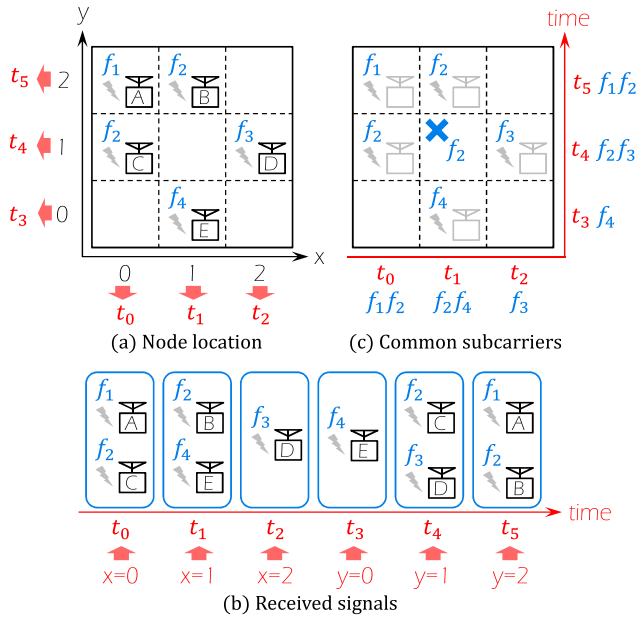
shows the common subcarriers in this case. For instance, the common subcarrier at $(1,2)$ is f_2 since f_2 is detected at both t_1 and t_5 mapped to $(1,2)$. To compare Fig. 5(a) with Fig. 5(c), it is obvious that the common subcarriers can contain redundancy in addition to the correct subcarriers sent by sensor nodes. There are no sensor nodes at $(1,1)$; nevertheless f_2 is received as the common subcarrier of the cell. The reason is that Node B and Node C among the same group select the same frequency f_2. Since Node B sends the subcarrier f_2 at t_1, t_5 and Node C sends the same subcarrier f_2 at t_0, t_4, the fusion center receives the subcarrier f_2 at t_1, t_4 that is also mapped to $(1,1)$, that is, the fusion center judges that the frequency component f_2 is sent at $(1,1)$ by mistake. If several sensor nodes at the same group select the same frequency, the common subcarriers may contain the extra subcarriers. Since the extracted information may include redundancy in addition to the correct data sent by sensor nodes, it is required to estimate the correct information.

2.3.2 AE Methods Based on Spatial Correlation

In this part, we describe AE methods by utilizing a spatial correlation of an observation object. If the distribution of the observation object has a spatial correlation, such as temperature and humidity, the information of extra common subcarriers is a value close to a sensed data across the cell over. Accordingly, an average value in a set of common subcarriers at each cell is estimated as the sensed data of each cell. When the distribution has a high spatial correlation, the information is estimated with high precision even if the extract information from the received signals includes a lot of redundancy. In addition, the fusion center has only to do averaging, that is, AE methods are very simple and have a low processing task. In AE method (1), the subject for estima-

tion is the cells where the common subcarriers are detected. Assuming that the fusion center knows the node location, the subject for estimation is the cells where sensor nodes are attached in AE method (2). So AE method (2) can estimate with higher precision than AE method (1) due to a low possibility of containing redundancy.
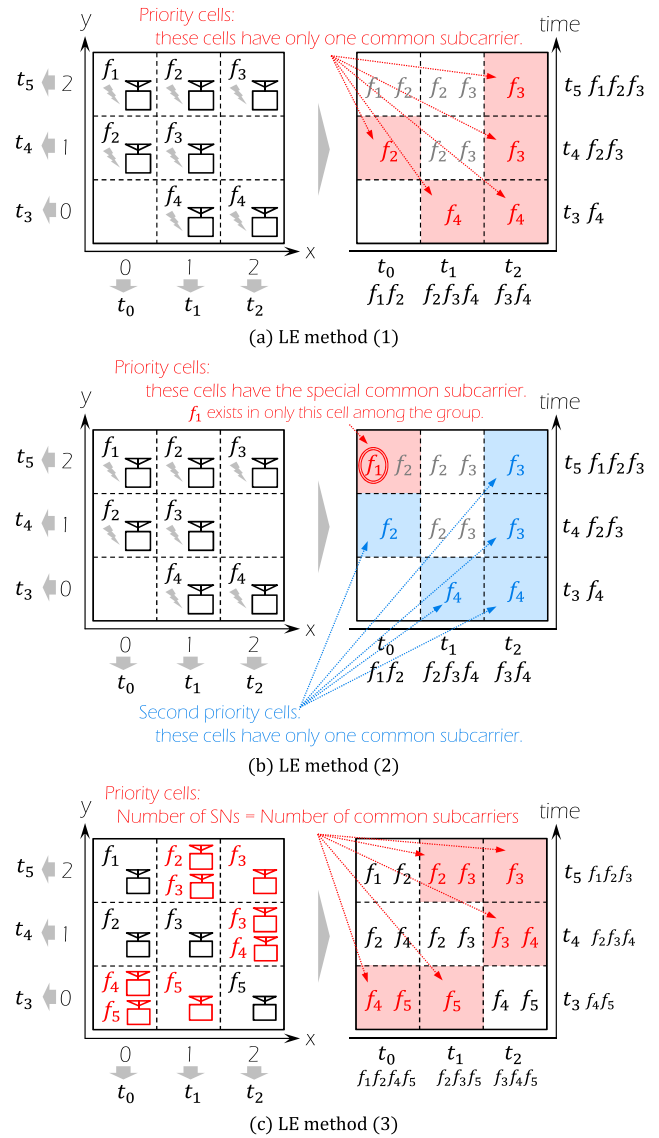
2.3.3 LE Methods Based on Positional Data

In this part, we describe LE methods by utilizing the node location. Now we suppose that more than one sensor node is not attached at the same cell. When several common subcarriers are detected at a cell, it is certain that the common subcarriers contain extra subcarriers besides that sent by the sensor node attached there. On the other hand, if only one common subcarrier is detected at a cell, the common subcarrier is likely to be sent by the sensor node attached there. By utilizing the pre-knowledge information, a certain specific

data is estimated as priority in LE methods. Figure 6 shows the priority cells, the subject for preferential estimation of each LE method. In LE method (1), the priority cells are the cells where only one common subcarrier is received. In Fig. 6(a), the data at (0,1) is estimated at first since the common subcarrier of (0,1) is only f_2. Similarly, (1,0), (2,0), (2,1), (2,2) are also the priority cells. In LE method (2), the priority cells are defined as the cells having the special common subcarrier that exists in only one cell among the group. When all preferential estimation of the priority cells is finished in LE method (2), the data of the cells where only one common subcarrier exists is estimated as second priority. Thus, the second priority cells of LE method (2) are equivalent to the priority cells of LE method (1). In Fig. 6(b), the data at (0,2) is estimated at first since the common subcarrier f_1 exists in only (0,2) among the group. The second priority cells are (0,1), (1,0), (2,0), (2,1), (2,2) where the number of common subcarriers of these cells is only one. Of course, these methods are effective only when one cell has one or few sensor nodes. On the other hand, LE method (3) is also useful when some sensor nodes are attached at the same cell. Supposed that the fusion center knows the node location, the data of the cells in which the number of sensor nodes matches the number of common subcarriers is preferentially estimated in LE method (3). In Fig. 6(c), the data at (0,0) is estimated at first since two sensor nodes are attached at (0,0) and two common subcarriers f_4, f_5 are received. Similarly, (1,0), (1,2), (2,1), (2,2) are the priority cells since the number of sensor nodes accords with the number of the common subcarriers at these cells. The process of LE methods is as follows.

   i. In each group, the data of the priority cells is estimated by the function shown in Eq. (4).

  ii. The common subcarriers used at Step i for the estimation are removed from the detected subcarriers at the time slots.

 iii. The new common subcarriers are rejudged.

 iv. Step i-iii are repeated until the priority cells do not exist in each group.

  v. If some new common subcarriers are detected at a cell, the sensed data of the cell is estimated as the average of values obtained from the new common subcarriers.

 vi. If the data of the cell that has the common subcarriers at the first judgment is not estimated, it is estimated as the average values obtained from the first common subcarriers.

Figure 7 shows the example of the estimating process in LE method (1). In this case, the sensed data of Nodes B,C,D,F,G is estimated at first. Then, the common subcarriers used at the first estimation are removed from the detected subcarriers. For example, the subcarrier f_2 sent by Node D is removed at t_0, t_4. At the second estimation, the data of Node A is estimated and there are no priority cells. Advancing to Step vi, the data of central cell is estimated as the average values obtained from the first common subcarriers f_2, f_4. In
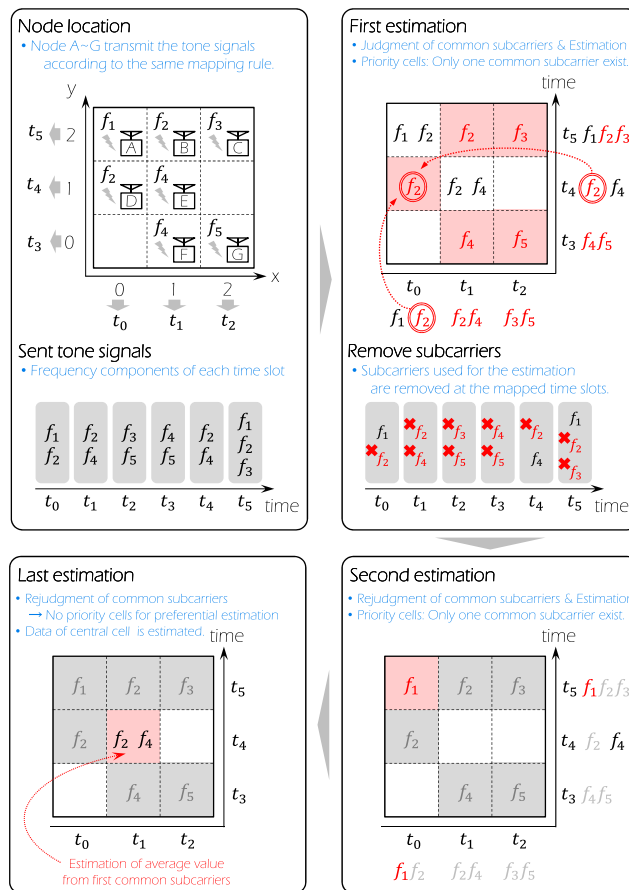
Fig. 7 Example of estimation using LE method (1).

Fig. 7, the data expect for Node E is correctly estimated.

3. Discussion of Performance

In this section, we discuss the performance of the proposed method. At the beginning, the relation between the spatial correlation of the observation object and the estimation accuracy of the proposed method is described. Next, we analyze the estimation precision in theory. At last, in terms of the period required for information gathering, the proposed method is compared with the standardized protocol.

3.1 Relation between Spatial Correlation and Accuracy

Figure 8 shows the relation between the spatial correlation of the observation object and the estimation accuracy of the proposed method. When the distribution of sensed data has high spatial correlation, that is, all sensor nodes in the same group send tone signals using the same frequency like Fig. 8(a), the extra data included by the received signals is coincided approximately with an actual sensed data. For example, the extra data of (1,2) coincides with the correct data that is actually sensed across the cell over. On the other hand, when the distribution has non-correlation, namely, all sensor nodes use different frequency like Fig. 8(c), the re-
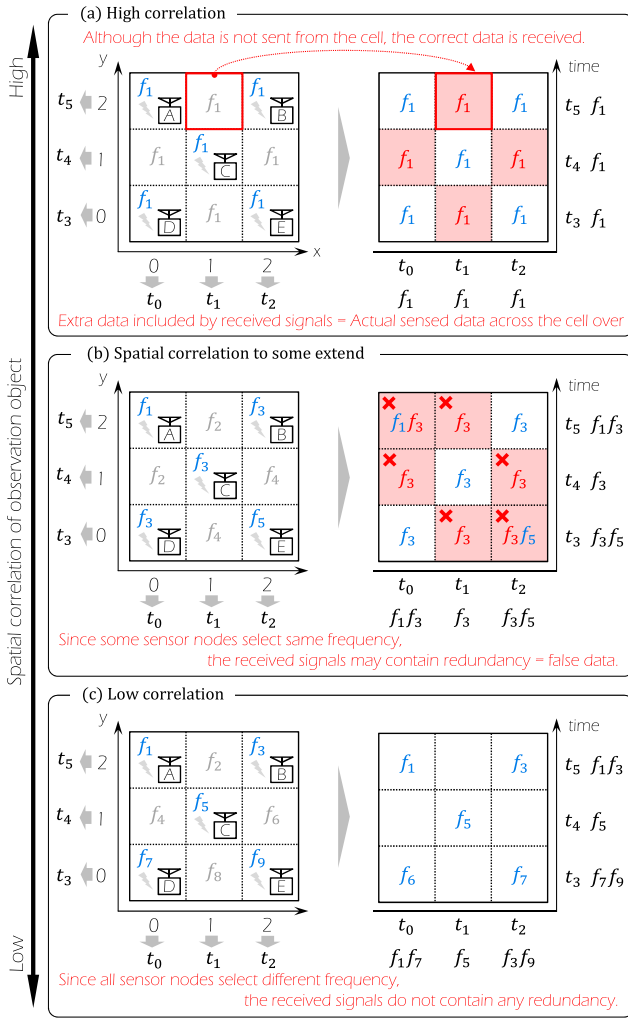
Fig. 8 Relation between correlation and accuracy.

Fig. 9 Including only correct data or not when Node A and Node B select the same frequency.

ceived data does not contain any redundancy. However, if the distribution has a correlation to some extent, several sensor nodes in the same group can select the same frequency. When the several sensor nodes are attached at the cells which vary in both coordinates like Fig. 8(b), the received signals contain the extra data. In other words, when the sensor nodes sensing the same value are attached at the cells which belong to the same group and vary in both coordinates, such as the case of sensing circular symmetric distribution, the extra information is included into the received signals even if the energy detection of the signals is perfect. It is possible that the estimation accuracy of the proposed method is enhanced by setting the cell size or the group size α into small value.

3.2 Theoretical Analysis

Here, we derive the probability of successful information received from all sensor nodes, P_n. This probability is defined as the ratio of the number of successful receiving all information sent by sensor nodes without extra information

to the all trials. Now, we suppose that n sensor nodes are allocated to one group, $\alpha \times \alpha$ cells. Then, each sensor node selects randomly one out of N_{car} subcarriers, that is, the probability of selecting a subcarrier is uniformly distributed and N_{car} denotes the number of subcarriers for frequency mapping, $N_{car} = N_{max} - N_{min} + 1$. If the transmitted information is shown in Fig. 8(b), the received signals contain the extra data. On the other hand, the received signals never contain the extra data in following two cases:

(A) All sensor nodes select different frequency. In this case, the extra information is not obtained regardless of the node location.

(B) When some sensor nodes select the same frequency, either x or y coordinate of these sensor nodes accord like Fig. 9 that shows each case of only correct data or not when Node A and Node B are attached at the same group and select the same frequency.

In the case of $n = 1$, the information can be correctly recovered, that is, $P_1 = 1$. In the cases of $n = 2$, the probability of non-received extra information is given by:

$$P_2 = \frac{N_{car} - 1}{N_{car}} + \frac{1}{N_{car}} \frac{2\alpha - 1}{\alpha^2}. \tag{5}$$

In Eq. (5), the first term is the probability that both sensor nodes select a different frequency. In the second term, $\frac{1}{N_{car}}$ is the probability that 2nd node selects the same frequency as 1st node. The number of cells that where x or y coordinate accord with that of 1st node is $(2\alpha - 1)$ in Fig. 9, and the number of cells composing one group is α^2, that is, $\frac{2\alpha-1}{\alpha^2}$ is the probability that 2nd node is attached at the cells where x or y coordinate accord with that of 1st node. Thus, each term of the Eq. (5) is the probability of the case (A) and case (B), respectively. In the case of $n = 3$, the probability P_3 is given by:

$$P_3 = \frac{N_{car} - 1}{N_{car}} \frac{N_{car} - 2}{N_{car}}$$
$$+ 3\left(\frac{N_{car} - 1}{N_{car}^2} \frac{2\alpha - 1}{\alpha^2}\right) + \left(\frac{1}{N_{car}} \frac{2\alpha - 1}{\alpha^2}\right)^2. \tag{6}$$

The first term of Eq. (6) means the probability of case (A). The second terms are the probability that two of three sensor nodes select a same frequency in the case (B). The third term is the probability that all sensor nodes select a same frequency in the case (B). According to above, P_n is given by:

$$P_n = \sum_{i=1}^{n} g(n,i) \times \frac{N_{\text{car}}!}{N_{\text{car}}^n (N_{\text{car}} - i)!} \times \left(\frac{2\alpha - 1}{\alpha^2} \right)^{n-i} \quad (7)$$

$$g(n,i) = \begin{cases} 1 & (i = 1) \\ \sum_{j_1=0}^{n-i} \sum_{j_2=0}^{j_1} \sum_{j_3=0}^{j_2} & \\ \cdots \sum_{j_{i-1}=0}^{j_{i-2}} 2^{j_1 - j_2} \times 3^{j_2 - j_3} \times \cdots \times i^{j_{i-1}} & (i \geq 2). \end{cases} \quad (8)$$

The function $g(n,i)$ denotes the total number of the combinations in dividing n sensor nodes into i groups as shown in Eq. (8). P_n is expressed by the sum of probability of case (B) when n sensor nodes select i of N_{car} subcarriers.

3.3 Time Efficiency

In terms of the period required for information gathering in WSN, the proposed method is compared with the standardized protocol, ZigBee/IEEE 802.15.4. Now, we consider the situation that n sensor nodes are attached in the sensing field, 12×12 cells, and send the temperature information in the range of $[20, 30]°$C with $0.1°$C precision.

In this situation, the period required for information gathering of ZigBee/IEEE 802.15.4 is as follows. The minimum header size of physical layer is 6 bytes [16]. We assume that the packet size of ZigBee is the summation of the header and the payload. The payload contains the sensed data (7 bit) and the positional data (4×2 bit) in this case. Thus, the packet size of ZigBee is 63 bits. The theoretical maximum data rate of ZigBee is 250 kbps. Supposed that all sensor nodes send data packets in turn without any collision and any time loss, the period T_{ZigBee} for gathering information from n sensor nodes is given by:

$$T_{\text{ZigBee}} = \frac{Packet\ size}{Data\ rate} \times Number\ of\ nodes$$
$$= \frac{63}{250} \times n\ [\text{ms}]. \quad (9)$$

Thus, T_{ZigBee} is increased in proportion to the number of sensor nodes in ZigBee.

The period of the proposed method is as follows: since the bandwidth of ZigBee is 2 MHz and 101 subcarriers are needed for the frequency mapping, the time slot length is defined as $25.5\,\mu$s. When each cell is simply mapped to a different time slot each, the period T_{simple} of the timing mapping required for 12×12 cells is given by:

$$T_{\text{simple}} = Time\ slot\ length \times Number\ of\ cells$$
$$= 25.5 \times 10^{-6} \times (12 \times 12) = 3.672\ [\text{ms}].$$
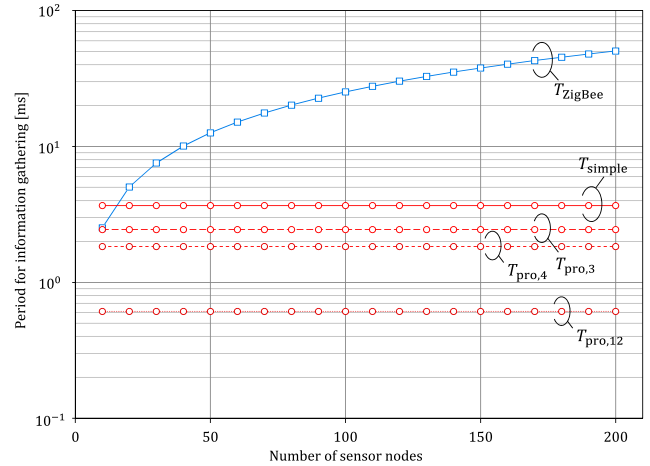
Fig. 10 Period required for information gathering.

Table 2 Period for information gathering ($n = 144$).

T_{ZigBee}	T_{simple}	$T_{\text{pro,3}}$	$T_{\text{pro,4}}$	$T_{\text{pro,12}}$
36.29 ms	3.672 ms	2.448 ms	1.836 ms	0.612 ms

Since the time compression rate is $\frac{2}{\alpha}$ in the case of partitioning into groups, the periodof the proposed method, $T_{\text{pro},\alpha}$ is given by:

$$T_{\text{pro},\alpha} = T_{\text{simple}} \times \frac{2}{\alpha} = 3.672 \times \frac{2}{\alpha}\ [\text{ms}]. \quad (10)$$

$T_{\text{pro},\alpha}$ has nothing to do with the number of sensor nodes unlike T_{ZigBee}.

In the condition of above, the period of each scheme are shown in Fig. 10. The proposed method can drastically shorten the period required for the all information gathering compared to ZigBee. When the fusion center gather information from 12×12 sensor nodes attached at 12×12 cells, the period of each scheme is shown in Table 2. As a result, the simple mapping shorten the period to roughly $\frac{1}{10}$ of Zig-Bee. Additionally, the larger group size α is, the more the period is shortened. In the case of $\alpha = 12$, the compression rate compared with ZigBee is the maximum, $\frac{1}{60}$ or less. In terms of the period for gathering, the proposed method is more effective for information gathering from multiple sensor nodes than the standardized protocol.

4. Simulation and Evaluation

4.1 System Model and Simulation Parameters

We perform the Monte Carlo simulation method to evaluate the precision of estimation when applying our proposed method. Simulation models are shown as follows. The fusion center is attached at the center of the sensing field. The sensor nodes are attached randomly in the field, sense the observation object, and send the information of own sensed data and positional data to the fusion center by transmitting the tone signals. The tone signals aggregating in

Table 3　Simulation parameters.

Definition	Setting
Channel model	Path loss, Log-normal shadowing, Multi-path fading
Decay constant	3
Standard deviation of shadowing	6 dB
Observation object	uniform distribution, temperature
Field size	12×12 m^2
Cell size	1×1 m^2
Gathered range of sensed target	$[0, 10], [20, 30]°C$
Average noise power	-120 dBm/subcarrier
Probability of false alarm	0.01
Averaging time	128
Transmission scheme	OFDM
Transmit power	0.1 mW/subcarrier

the Rayleigh fading channel, the fusion center receives the tone signals. The observation object is categorized into two types. One is distributed as uniform distribution in the range of $[0, 10]$. The other one is the temperature distribution in the range of $[20, 30]°C$: the heat source of $30°C$ is arranged in the field in which the heat does not reflect and spread equally from the source to all direction. Now we suppose that the synchronization of frequency and time are perfect among the all sensor nodes and the fusion center. The other detail parameters are shown in Table 3.

4.2　Simulation Results

4.2.1　Relation between Precision and Group Size

Figure 11 shows the rate of receiving only the correct data sent by sensor nodes in the case of sensing the uniform distribution. The rate means P_n defined as the ratio of the number of successful receiving all information sent by n sensor nodes without extra information for in all trials. Although we assume that the energy detection is perfect in the theoretical analysis, the results of the simulation give good agreement with the theoretical value obtained by Eq. (7) in Fig. 11. That is because the received power of the subcarriers is enough to detect due to the small distance between the fusion center and the sensor nodes. As a result of Fig. 11, the estimation accuracy of the proposed method is not influenced by the radio propagation and noise in setting the probability of false alarm into 0.01.

In the case of $\alpha = 3$, the rate of perfectly successful gathering is over 80%. In comparison with the case of $\alpha = 3$, the rate is lower in the case of $\alpha = 4$. The reason is that the larger the group size α is, the more sensor nodes among the same group select a same frequency, namely, the probability that the common subcarriers contain the false data expect for correct data sent by sensor nodes increases. While the larger α is, the shorter it can take time to gather information due to the time compression rate $\frac{2}{\alpha}$, the lower the precision of gath-
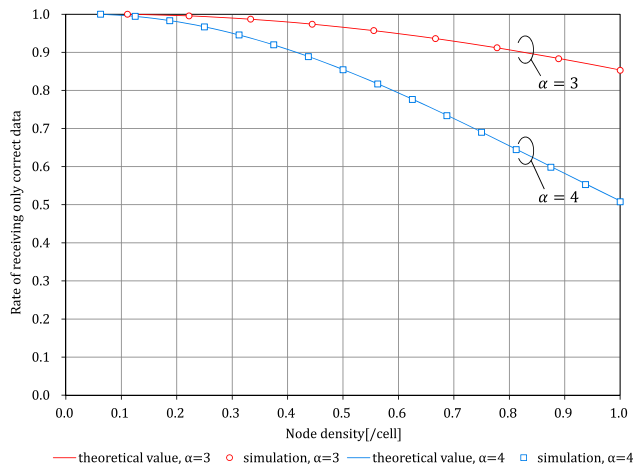
Fig. 11　Rate of reveiving only correct data.
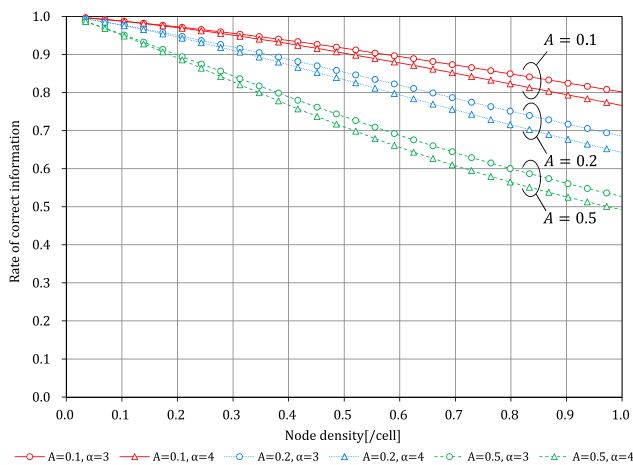
Fig. 12　Rate of information where only correct data is received under random node location.

ered data is: to sum up, there is the trade-off between the time compression and the estimation accuracy of the gathered data. In the proposed method, the fusion center cannot always gather all information with good accuracy. Therefore, it is required to estimate the correct information using AE methods or LE methods. We discuss the effectiveness of each estimation method in Part 4.2.3.

4.2.2　Relation between Precision and Quantization Level

Figure 12 shows the rate of the information at the cells in which only correct subcarriers sent by sensor nodes are detected as the common subcarriers in the case of sensing the temperature distribution. In the case of sensing the temperature distribution as well as the uniform distribution, the smaller the group size α is, the higher the rate of the correct information becomes. Then, the case of $A = 0.1°C$ is the highest rate of the information at the cells where the only correct information is received. This is because the smaller the quantization level of sensed data is, the fewer sensor nodes select the same frequency, and the lower the

probability that the common subcarriers contain the false data becomes. In Fig. 12, the number of subcarriers for the frequency mapping is 101, 51, 21 in each case of $A = 0.1, 0.2, 0.5$°C. Since the overlap of the frequency selected by sensor nodes is increased, the performance of $A = 0.5$°C deteriorates. Therefore, there is the trade-off between the number of subcarriers and the precision of gathered data.

4.2.3   Comparison with Estimation Methods

Figure 13 shows the rate of the information estimated as the correct information sent by sensor nodes. Figure 14 shows the average error of temperature per cell. In all methods, the average error is lower than 0.08°C in Fig. 14. Moreover, in Fig. 13, over 80% of the information sent by sensor nodes is estimated correctly in all estimation methods besides LE method (2). Therefore we can gather the information with high precision in a short time by using the proposed methods.

In LE method (3), the information is estimated with the highest precision. This is because the fusion center utilizes the node location effectively. Since the information of the priority cells in which the number of sensor nodes matches the number of common subcarriers is preferentially

estimated in LE method (3), the fusion center can obtain the more information sent by sensor nodes. In AE method (2), the information is estimated with the second highest precision. This is because the observed distribution of temperature has a spatial correlation. Furthermore, the fusion center utilizes the node location and estimates only the average observed values of the cells in which the sensor nodes are attached in AE method (2). Since the average values of all cells that have common subcarriers in AE method (1), the precision of AE method (1) is lower than that of AE method (2). The precision of LE methods (1) and (2) is lower than the others. The reason is that the sensor nodes are located randomly; that is the cells can have multiple sensor nodes. In LE methods (1) and (2), the fusion center estimates preferentially the information of the cells that have only one common subcarrier or special common subcarrier. Therefore, these methods cannot avoid the situation that the cells can have more than one sensor node. Figures 15 and 16 show the rate of the information that is estimated as the correct information sent by the sensor nodes and the average error of temperature, respectively, when sensor nodes are attached randomly in the condition that one cell has one or few sensor node. In all methods, the estimation precision is raised compared with the case of random location in Figs. 13 and 14. Over 90% of the information sent by sensor nodes is estimated correctly in Fig. 15, and the average error is lower than 0.03°C in Fig. 16. The precision of LE methods (1) and (2) is approximately equal to that of LE method (3), so these methods are useful under the condition.

From above simulation result, the location information of sensor nodes contributes to the estimation. The effective situations of each method are shown in Table 4. LE method (3) that utilizes the location information achieves the highest performance among the five methods. Under the limited calculation processing of the fusion center, AE method (2) is effective. On the other hand, when the node density per cell is low without the location information, the performance of LE method (1) and LE method (2) is equivalent to that of LE method (3). When the distribution of the observation object has a spatial correlation under the limited processing
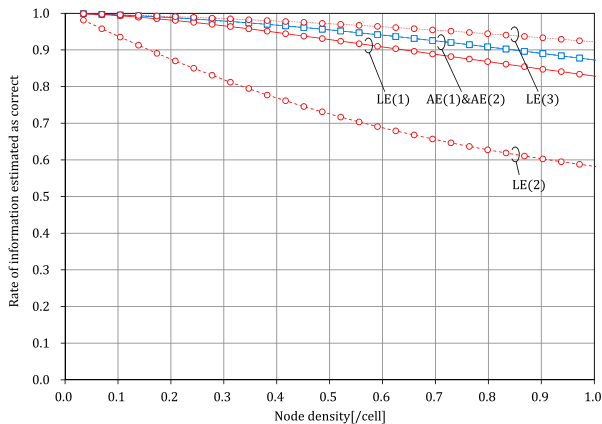
Fig. 13   Rate of correct information under random node location.
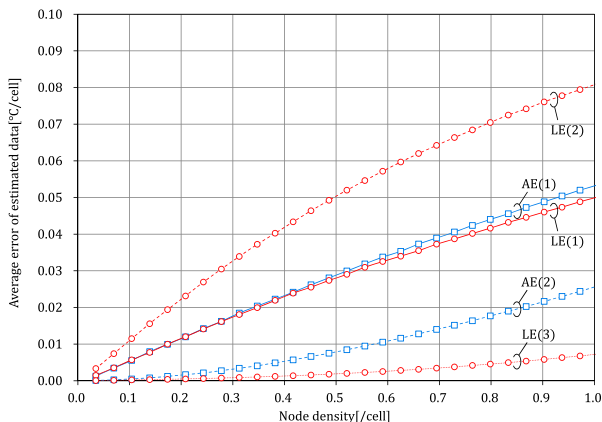
Fig. 14   Average error of estimated data under random node location.
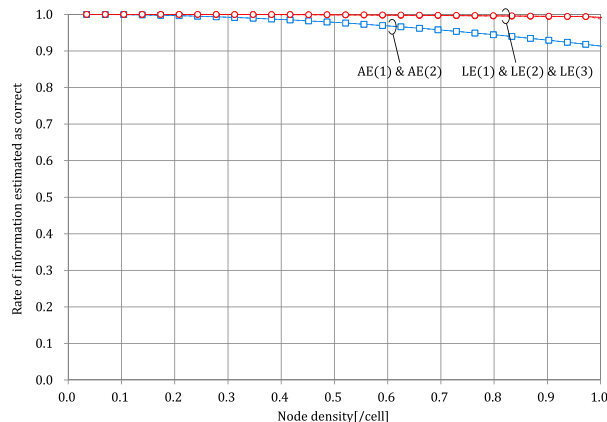
Fig. 15   Rate of correct information under limited node location.
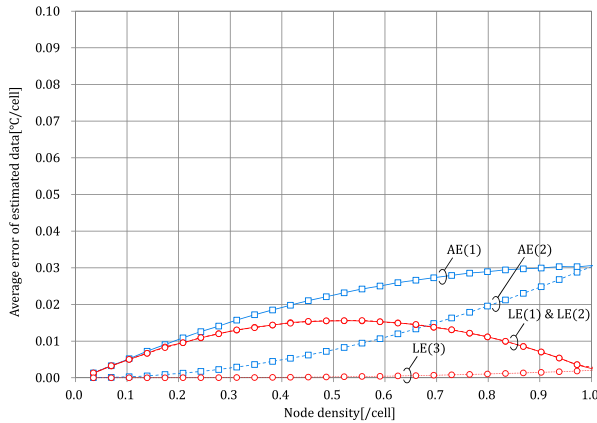
Fig. 16   Average error of estimated data under limited node location.

Table 4   Effective situations of each estimation method.

Location information	√	√	-	-
Limited processing	-	√	√	-
Spatial correlation	-	√	√	-
Low density	-	-	-	√
Effective method	LE (3)	AE (2)	AE (1)	LE (1) LE (2)

without the location information, AE method (1) that is the simplest method is effective.

5. Conclusion

In this paper, we presented a novel information gathering and estimating methods for WSNs. In the proposed method for information gathering, each sensor node converts sensed data to a subcarrier of OFDM signals (frequency-axis) and turns positional data into two time-slots (time-axis). The fusion center receives the tone signals and estimates the correct information from frequency and timing of received signals. The proposed method only requires simpler communication than the standardized methods based on packets communications. As a result, the proposed method is expected to shorten the period required to gather information and to reduce the processing task and the battery power consumption of each sensor node. Although the proposed method has the above advantage, it is possible that the received signals include false data in addition to data sent by sensor nodes. Thus, we also proposed the five methods for information estimation in this paper. In AE methods, the average values got from the common subcarriers of each cell is estimated as sensed data value in the cell by utilizing a spatial correlation. In LE methods (1) and (2), the fusion center estimates preferentially the information of the cells that have only one common subcarrier or special common subcarrier. In LE method (3), the information is preferentially estimated at the cell in which the number of sensor nodes matches the number of common subcarriers. By using the proposed methods, we can gather two-dimensional distribution of the tempera-

ture with high precision in a short time.

References

[1] I.F. Akylidiz, W. Su, Y. Sankarasubramaniam, and E. Cayirci, "A survey on sensor networks," IEEE Commun. Mag., vol.40, no.8, pp.102–114, Aug. 2002.

[2] R. Rajagopalan and P.K. Varshney, "Data aggregation techniques in sensor networks: A survey," IEEE Commun. Surveys and Tutorials, vol.8, pp.48–63, 2006.

[3] V.C. Gungor, B. Lu, and G.P. Hancke, "Opportunities and challenges of wireless sensor networks in smart grid," IEEE Trans. Ind. Electron., vol.57, no.10, pp.3557–3564, Oct. 2010.

[4] L. Filipponi, A. Vitaletti, G. Landi, V. Memeo, G. Laura, and P. Pucci, "Smart city: An event driven architecture for monitoring public spaces with heterogeneous sensors," Proc. 4th IEEE Int. Conf. Sensor Technol. Appl., pp.281–286, July 2010.

[5] G. Tolle and W. Hong, "A macroscope in the redwoods," ACM SenSys, pp.51–63, 2005.

[6] L. Selavo and J. Porter, "LUSTER: Wireless sensor network for environmental research," ACM SenSys, pp.103–116, 2007.

[7] M. Ohta, T. Fujii, K. Muraoka, and M. Ariyoshi, "A novel method for information gathering by using orthogonal narrowband signal for cooperative sensing in cognitive radio," IEICE Trans. Commun., vol.E92-B, no.12, pp.3625–3634, Dec. 2009.

[8] T. Fujii, T. Endou, and M. Ohta, "High efficient multiple sensing information gathering for wireless sensor networks," Proc. ICUFN2013, pp.202–207, Da Nang, Vietnam, July 2013.

[9] S. Sakai, T. Endou, and T. Fujii, "Frequency assigned information gathering method for motion-capture in Wireless Sensor Networks," Proc. ICUFN2013, pp.208–213, Da Nang, Vietnam, July 2013.

[10] T. Endou and T. Fujii, "Real time information gathering based on frequency and timing assignment for wireless sensor networks," Proc. ICCS2012, pp.167–171, Singapore, Nov. 2012.

[11] B. Sundararaman, U. Buy, and A.D. Kshemklyani, "Clock synchronization in wireless sensor networks: A survey," Ad hoc Networks, vol.3, no.3, pp.281–323, 2005.

[12] J. Elson, L. Girod, and D. Estrin, "Fine-grained network time synchronization using reference broadcasts," Proc. 5th Symp. Operating Systems Design and Implementation (OSDI 2002), pp.143–163, Boston, MA, Dec. 2002.

[13] S. Ganeriwal, R. Kumar, and M. Srivastava, "Timing-sync protocol for sensor networks," Proc. 1st ACM Conference on Embedded Networked Sensor Systems. pp.138–149, Los Angeles, CA, 2003.

[14] T.M. Schmidl and D.C. Cox, "Robust frequency and timing synchronization for OFDM," IEEE Trans. Commun., vol.45, pp.1613–1621, Dec. 1997.

[15] H.K. Song, Y.H. You, J.H. Paik, and Y.S. Cho, "Frequency-offset synchronization and channel estimation for OFDM-based transmission," IEEE Commun. Lett., vol.4, pp.95–97, March 2000.

[16] J.S. Lee, Y.W. Su, and C.C. Shen, "A comparative study of wireless protocols: Bluetooth, UWB, ZigBee, and Wi-Fi," Proc. IEEE 33rd Annu. Conf. IECON, pp.46–51, Nov. 2007.

Tomomi Endou   was born in Chiba, Japan, in 1989. She received the B.S. and M.S. degrees in The University of Electro-Communications, Japan, in 2012 and 2014. Her research topic is data aggregation for wireless sensor networks.

Shunta Sakai   was born in Tokyo, Japan, in 1990. He received the B.S. and M.S. degrees in The University of Electro-Communications, Japan, in 2013 and 2015, respectively. He is currently a master course student of The University of Electro-Communications, Japan. His research topic is information gathering for wireless sensor networks.

Takeo Fujii   was born in Tokyo, Japan, in 1974. He received the B.E., M.E. and Ph.D. degrees in electrical engineering from Keio University, Yokohama, Japan, in 1997, 1999 and 2002 respectively. From 2000 to 2002, he was a research associate in the Department of Information and Computer Science, Keio University. From 2002 to 2006, he was an assistant professor in the Department of Electrical and Electronic Engineering, Tokyo University of Agriculture and Technology. From 2006 to 2014, he has been an associate professor in Advanced Wireless Communication Research Center, The University of Electro-Communications. Currently, he is a professor in Advanced Wireless and Communication Research Center, The University of Electro-Communications. His current research interests are in cognitive radio and ad-hoc wireless networks. He received Best Paper Award in IEEE VTC 1999-Fall, 2001 Active Research Award in Radio Communication Systems from IEICE technical committee of RCS, 2001 Ericsson Young Scientist Award, Young Researcher's Award from the IEICE in 2004, The Young Researcher Study Encouragement Award from IEICE technical committee of AN in 2009, and Best Paper Award in IEEE CCNC 2013. He is a member of IEEE.